

Semiclassical action based on dynamical mean-field theory describing electrons interacting with local lattice fluctuations

Stefan Blawid and Gertrud Zwirnagl

Institut für Mathematische Physik, TU Braunschweig, Mendelssohnstr. 3, 38106 Braunschweig
(November 13, 2018)

We extend a recently introduced semiclassical approach to calculating the influence of local lattice fluctuations on electronic properties of metals and metallic molecular crystals. The effective action of electrons in degenerate orbital states coupling to Jahn-Teller distortions is derived, employing dynamical mean-field theory and adiabatic expansions. We improve on previous numerical treatments of the semiclassical action and present for the simplifying Holstein model results for the finite temperature optical conductivity at electron-phonon coupling strengths from weak to strong. Significant transfer of spectral weight from high to low frequencies is obtained on isotope substitution in the Fermi-liquid to polaron crossover regime.

71.10.-w, 71.30.+h, 71.10.Fd

I. INTRODUCTION

Despite many years of research, techniques to calculate the influence of strong vibronic interactions on electronic properties of metals and metallic molecular crystals are urgently needed. Strong couplings of conduction electrons to local lattice fluctuations have been observed in certain phonon mediated superconductors with high transition temperatures and manifest themselves among other effects in unexpected mid-infrared transitions in the optical conductivity in these materials, like in $\text{Ba}_{1-x}\text{K}_x\text{BiO}_3$ ¹ and in the alkali-doped C_{60} fullerenes.^{2,3} Standard Migdal Eliashberg (ME) theory⁴ is not sufficient to explain these phenomena although typical phonon frequencies of physical interest may remain small compared to typical electron energies. The reason for the failure is that ME theory assumes that the underlying electronic ground state can be described by Fermi liquid theory. However, if the electron-lattice coupling strength $\lambda = \Lambda/t$ exceeds a critical value (of order unity) the conduction electrons are believed to form “small polarons”,⁵ so that the electronic groundstate is fundamentally reconstructed.

Signatures of polaronic behavior have been most accurately studied in the case of one or few electrons employing the Lang-Firsov transformation.⁶ However, its applicability to the physically relevant case of metallic densities is not established. A suitable method to study the interaction of conduction electrons with *local* lattice fluctuations may be the dynamical mean-field theory⁷ and in recent years an increasing number of studies have been published. In spite of the substantial simplifications which occur when the conduction electrons are described by local fluctuating fields the resulting equations are still very complicated. An exact solution is only possible in the case of a single polaron.⁸ Numerically “exact” solutions are available using quantum Monte Carlo methods⁹ in the antiadiabatic limit $\Omega \sim t$ of unclear physical rele-

vance and using numerical renormalization techniques¹⁰ at zero temperature. Especially the latter is a promising approach at least for simplifying models like the Holstein model and may be extended in future to finite temperatures. Semianalytical techniques have the advantage of being instructive and of being extensible to more realistic model systems of conduction electrons coupling to local lattice distortions including maybe even electron-electron interactions. These approaches^{11–14} rely on a detailed analysis of the effective action based on the dynamical mean-field theory.

Here, we extend a “semiclassical” approach¹⁴ recently introduced by one of the authors to general models of electrons in degenerate orbital states coupling to Jahn-Teller distortions. The classical (static) phonon modes are treated exactly and the quantum (dynamical) modes are expanded to second order. The adiabatic expansion of the classical action allows for treating polaronic effects in the physical relevant limit of small adiabatic parameter, from weak to strong electron-phonon couplings. However, the method is restricted to temperatures which exceed or are comparable to an energy scale set by a renormalized phonon frequency. Numerically, the method is implemented for the simplifying Holstein model of (spinless) electrons at half filling. We resolve previous numerical restrictions¹⁴ connected with the analytic continuation of the local electronic Green function from the imaginary to the real frequency axis which allows for a more complete understanding of dynamical quantities, especially the optical conductivity. A treatment of coupling strengths beyond the classical polaronic instability becomes numerically tractable. Pioneering work in the calculation of the density of states and the optical conductivity at low temperatures has been done by Benedetti and Zeyher¹² and we provide a comparison to their results. The remainder of the paper is organized as follows. In Sec. II we apply the dynamical mean-field theory to models of metallic molecular crystals or metals with strong Jahn-Teller distortions. The polaronic

instability for classical vibrations is discussed in Sec. III and known results in the opposite quantum limit at zero temperature are reviewed in Sec. IV. Section V gives the adiabatic expansion of the effective action and discusses the numerical implementation to treat the Holstein model at half-filling, as well as the limitations of the approach. Numerical results for the density of states and the optical conductivity are presented and discussed extensively. We conclude in Sec. VI.

II. MODELLING

We study metallic molecular crystals whose Hamiltonians are described by

$$H = \sum_i H_i^{\text{Molecule}} + \sum_{i,j,\alpha,\beta} t_{ij}^{\alpha\beta} c_{i\alpha}^\dagger c_{j\beta} - \mu \sum_{i,\alpha} c_{i,\alpha}^\dagger c_{i,\alpha}. \quad (1)$$

Here, the operator $c_{i\alpha}^\dagger$ creates an electron in the molecular orbital (MO) α on the i -th molecule. For simplicity we suppress the spin index and consider spinless electrons. However, our treatment can be easily extended to a paramagnetic state by including the appropriate spin degeneracy. We will assume that the molecular orbital states are single particle like, e.g. provided by a Hartree-Fock treatment of the molecule. In particular, the hopping of electrons on and off a molecule shall not alter the local electronic level scheme. In this respect the assumption of spinless electrons helps to avoid unphysical large fluctuations in the local occupation number of the partially filled MOs giving rise to the conduction bands.

In general, the high local symmetry of a molecule will lead to an orbital degeneracy of the interesting, partially filled MOs. Therefore H_{Molecule} describes the coupling between a f -fold degenerate electronic term and N Jahn-Teller active modes

$$H_{\text{Molecule}} = \frac{1}{2} \sum_{i=1}^N (K Q_i^2 + M \dot{Q}_i^2) + \begin{pmatrix} W_{11}(Q_1, \dots, Q_N) & \cdots & W_{1f} \\ \vdots & \ddots & \vdots \\ W_{f1} & \cdots & W_{ff} \end{pmatrix}. \quad (2)$$

Here, the Q_i denote the normal coordinates of the Jahn-Teller distortions. According to the Jahn-Teller theorem the leading term of the coupling constants W_{ij} is linear in Q and different matrix elements are symmetry related. Employing group theory we may characterize different cases according to different irreducible representations of all possible point groups. In particular $E \otimes e$ denotes the coupling of a double degenerated electronic term with two Jahn-Teller modes.

We do not attempt to solve (1) directly which is a very difficult problem. Instead we are analysing an *effective action* of the form

$$S_{\text{eff}} = \frac{1}{2T} \sum_{i=1}^N \sum_k Q_i(\omega_k) (K + M\omega_k^2) Q_i(\omega_{-k}) - \mu n - \text{Tr}_n \text{Tr}_{\text{orb}} \ln \left\{ c(\nu_n) - \underline{W}[\tilde{Q}(\nu_n - \nu_m)] \right\}. \quad (3)$$

This is the action of a single molecule embedded in an effective environment when the fermionic fields (which occur in quadratic form) are integrated out. The latter give rise to the mean-fields $c(\nu_n)$ which describe the conduction electrons and depend on odd Matsubara frequencies $\nu_n = 2\pi T(n + 1/2)$. The $Q_i(\omega_k)$ are bosonic fields (describing the Jahn-Teller modes) depending on even Matsubara frequencies $\omega_k = 2\pi T k$. Note that the \underline{W} -term in the logarithm is nondiagonal in both the Matsubara and the orbital index. The action S_{eff} arises in a *dynamical mean-field* (DMFT)⁷ description of the original lattice model Eq. (1) if we assume a structureless and fast fluctuating environment of a single molecule, i.e. if the local Green function can be averaged over the $f = n_{\text{orb}}$ orbital degrees of freedom

$$\mathcal{G} = \frac{1}{n_{\text{orb}}} \text{Tr}_{\text{orb}} \underline{G}_{\text{loc}}. \quad (4)$$

The orbital averaging was first introduced in Ref. 11. The DMFT treatment provides a self-consistency expression for the dynamic mean-fields c . The partition function may be written as a functional integral over the bosonic fields

$$Z = \int \mathcal{D}[Q] \exp(-S_{\text{eff}}). \quad (5)$$

from which the local Green function \mathcal{G} follows

$$\mathcal{G}(\nu_n) \equiv \frac{\delta \ln Z}{\delta c(\nu_n)}. \quad (6)$$

The molecules are arranged on a three dimensional lattice. However, after averaging over the orbital degrees of freedom in (4) it may be sufficient to work with an effective density of states of simple form, e.g. semicircular $\rho_0(\epsilon) = (1/N) \sum_k \delta(\epsilon - \epsilon_k) = 1/(2\pi t^2) \sqrt{4t^2 - \epsilon^2}$. In this case the self-consistency equation (4) can be written in the form

$$c_n = i\omega_n + \mu - \frac{t^2}{n_{\text{orb}}} \mathcal{G}_n(\{c_n\}). \quad (7)$$

Eqs. (3), (5), (6) and (7) form a complete set of equations which, in principle, can be solved for the orbital averaged local Green function on the imaginary axis of a molecular crystal with Jahn-Teller active local distortions. However, one cannot evaluate the path integrals exactly in Eq. (5) and further approximations are necessary. We adopt the adiabatic expansion of the effective action Eq. (3) which includes the leading term in the non diagonal part of the electron-phonon interaction as discussed in Sec. V.

The present modelling is not restricted to the description of metallic molecular crystals as pioneering works on the “colossal magnetoresistance” manganites demonstrate.¹¹ However, when applying the present formalism to others than molecular crystals one have to keep in mind that local distortions of the crystal unit cell do influence the neighboring cells. In particular, in transition metal oxides E_g symmetry distortions of the oxygen octahedra move oxygen atoms of several unit cells. Therefore, in this case the presented modelling is only applicable to phenomena which involve incoherent features of the electronic Green function, i.e. which involve high temperatures or high frequencies.

III. CLASSICAL ACTION: ANALYTICAL INSIGHTS

A good starting point to gain some insight in the physics described by the Eqs. (3) - (7) is to analyse the effective action Eq. (3) in the high temperature limit¹¹ when only thermal fluctuations are present. S_{eff} reads

$$S_{\text{class}}(\vec{Q}) = \frac{K}{2T} \sum_{i=1}^N Q_i^2 - \mu n - \text{Tr}_n \text{Tr}_{\text{orb}} \ln \left\{ c(\nu_n) - \underline{\underline{W}}[\vec{Q}] \right\} \quad (8)$$

where the $Q_i = Q_i(\omega_k = 0)$ are the classical components of the bosonic fields. The function

$$P(\vec{Q}) = \exp[-S_{\text{class}}(\vec{Q})] \quad (9)$$

is the (unrenormalized) probability that the classic Jahn-Teller distortion takes the value \vec{Q} .

We specialize now to different cases. The case of a non degenerate electronic term coupling to a totally symmetric distortion (Holstein model) is the simplest situation with the interaction matrix being a scalar $\underline{\underline{W}} = gQ$. The strength of the electron-phonon coupling is measured by $\Lambda = g^2/K$. (In the following we will frequently denote the dimensionless coupling parameter by $\lambda = \Lambda/t$). It is easy to show¹¹ that the effective action $S_{\text{class}}(Q)$ changes from a single to a double well behavior with increasing Λ as shown in Fig.1. In Fig.1 the term $-Q/2$ has been added to the effective action to symmetrize the distortions in the case of hole and electron occupation on a given site. A double well occurs when the Q^2 -coefficient in the effective action vanishes. This is the case for $\Lambda_c = -1/\Gamma_2$ with

$$\Gamma_2 = T \sum_n c^{-2}(\nu_n). \quad (10)$$

Here the fully self-consistent determined dynamical fields have to be used. If we insert the free form, the critical electron-phonon coupling reads¹⁵:

$$\Lambda_c = \frac{3\pi}{4} [1 - (\mu/2t)^2]^{-3/2}. \quad (11)$$

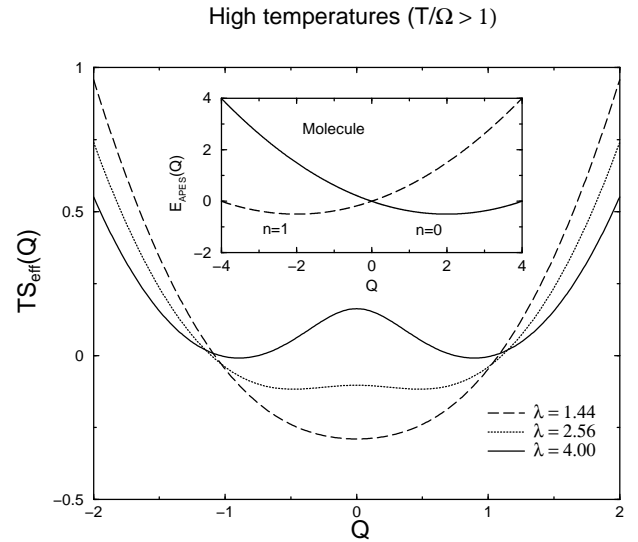


FIG. 1. MAIN PANEL: The (classical) effective action S_{eff} as function of the distortion Q for the Holstein model at half-filling. Shown is the behavior for different coupling strengths λ at a high temperature of $T/t = 0.2$. The forming of a double well at a finite value of λ is clearly seen. INSET: Adiabatic potential energy surface $E_{\text{APES}}(Q) = Q^2/2\Lambda + Q(n-1/2)$ at $\lambda = 2.56$ for a molecule with no and one electron in the relevant molecule orbital. The distortion equals $\pm\lambda$.

At couplings exceeding Λ_c the motion of an electron is accompanied by a lattice distortion, i.e. small polarons are formed. It is important to note that the behavior of an isolated molecule is different. With a linear electron-phonon coupling a finite Jahn-Teller distortion occurs for every finite coupling constant Λ as illustrated in the inset of Fig.1. In a crystal the quantum fluctuations of the occupation numbers of the MOs due to the hopping of the electrons smear out this distortion. A finite minimal coupling strength is required for the lattice relaxing to the actual occupation of a given site.

The occurrence of finite Jahn-Teller distortions at a finite critical value of Λ is a generic feature of the classical action S_{class} . However, the critical value depends upon details of the Jahn-Teller coupling, in particular upon the degeneracy of the problem. This can be illustrated by comparing the $T_1 \otimes h$ -problem describing the coupling between electrons and vibrations of the charged C_{60} molecules to the $E \otimes e$ -problem relevant for transition metal oxides with perovskite structure. Electrons added to an isolated fullerene molecule belong to the T_{1u} lowest unoccupied MO which can couple linearly to vibrations of symmetry h_g .¹⁶ The Jahn-Teller interaction matrix reads

$$\underline{\underline{W}} = \frac{g}{2} \begin{pmatrix} Q_1 - \sqrt{3}Q_4 & -\sqrt{3}Q_3 & -\sqrt{3}Q_2 \\ -\sqrt{3}Q_3 & Q_1 + \sqrt{3}Q_4 & -\sqrt{3}Q_5 \\ -\sqrt{3}Q_2 & -\sqrt{3}Q_5 & -2Q_1 \end{pmatrix}. \quad (12)$$

When introducing a new parametrization and expressing Q_1, \dots, Q_5 via one amplitude Q and four angles¹⁶ the

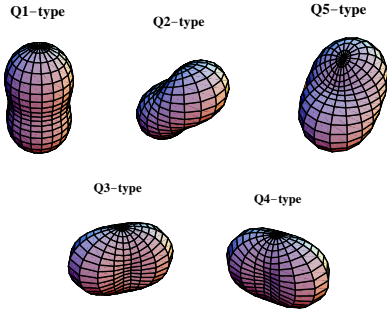


FIG. 2. The five h -type Jahn-Teller distortions measured relative to a sphere.

classical effective action can be written in compact form

$$S_{\text{eff}} = \frac{Q^2}{2\Lambda T} - \text{Tr}_n \ln \left[c^3(\nu_n) - \frac{3}{4} Q^2 c(\nu_n) + \frac{Q^3}{4} \cos 3\alpha \right]. \quad (13)$$

Expanding S_{eff} for small Q reveals that the Q^2 -coefficient of the classical action vanishes for

$$\Lambda_c = -\frac{2}{3} \frac{1}{\Gamma_2}. \quad (14)$$

For coupling strengths $\Lambda > \Lambda_c$ finite Jahn-Teller distortions occur as displayed in Fig. 2. For the $E \otimes e$ -problem one obtains¹¹ $\Lambda_c = -1/2\Gamma_2$. We see that for comparable values of the “electron bubbles” Γ_2 the occurrence of finite Jahn-Teller distortions require stronger electron-phonon couplings in the higher degenerate case. In this sense the weak-coupling regime for the $T_1 \otimes h$ -problem extends to larger coupling strengths.

It is important to note that the occurrence of a polaronic instability indicates a break down of Migdal-Eliashberg theory because the ground state is fundamentally reconstructed. Physically speaking a quasiparticle picture does not hold in the transition regime because neither a description as electrons nor as polarons is valid. This give rise to interesting isotope effects on electronic properties as discussed in Ref. 14 and in Sec. V.

IV. INFLUENCE OF QUANTUM FLUCTUATIONS

Quantum fluctuations of the lattice will change the value of the coupling constant λ_c needed to form small polarons. Even for stronger electron phonon couplings when a classical lattice would adjust to the occupancy of a given site, possible tunneling may hinder the formation of polarons or even prevent it. At sufficiently low temperatures only zero-point quantum vibrations of the lattice are present and the classical picture is not valid. Detailed studies exist^{10,12,15} for the evolution of the electronic effective mass in the Holstein model as function of

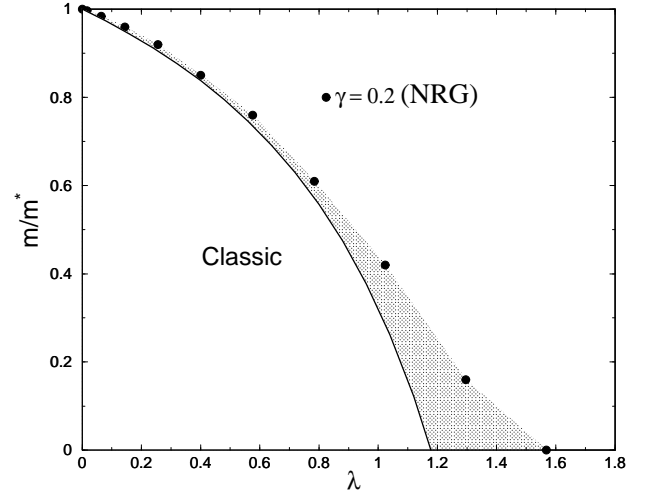


FIG. 3. Inverse ratio of the effective and bare electronic mass as function of λ . The classical prediction is compared to the results obtained from an NRG study by Meyer, Hewson and Bulla in Ref. 10 at finite phonon frequency. In the shaded parameter regime strong isotope effects have to be expected.

the coupling strength Λ in the adiabatic regime. All results indicate that the electronic effective mass diverges (or at least increases very rapidly) at a *finite* value of the electron phonon coupling even in the presence of zero-point fluctuations. In Fig. 3 we replot the results of a numerical renormalization (NRG) study published in Ref. 10. The inverse ratio of the effective and bare electronic mass as function of Λ ($= 2g^2/\omega_0$ in the notations of Ref. 10) is shown. For the adiabatic parameter $\gamma = \Omega/t = 0.2$ ($t = 0.25$) a critical value of $\lambda_c(\gamma) \approx 1.57$ has been reported. The classical approach predicts $m^*/m = 1 + \bar{\Lambda} \rho(\mu)$ with $\bar{\Lambda} = \Lambda/(1 - \Lambda/\Lambda_c)$, i.e. a diverging electron mass at the classical value Λ_c which reads for a semicircular density of states at half filling $\Lambda_c = 3\pi t/[(2s+1)4]$. The classical result is also shown in Fig. 3. Note that in the NRG investigations the case of twofold spin degeneracy is considered, i.e. the classical polaronic instability occurs at $\lambda_c \approx 1.18$. We conjecture that with increasing values of the phonon frequency the “polaronic instability” is shifted to larger values of the electron phonon coupling and in the shaded parameter regime of Fig. 3 strong isotope effects on electronic properties have to be expected.

If one includes the leading frequency correction to the finite loop (ME) diagram, the effective mass reads¹⁵

$$\frac{m^*}{m} = 1 + \bar{\Lambda} \rho(\mu) - \frac{1}{4} \bar{\Lambda} \bar{\gamma} \quad (15)$$

with $\bar{\gamma}$ being the renormalized adiabatic parameter $\bar{\gamma} = \gamma \sqrt{1 - \Lambda/\Lambda_c}$. Therefore, the electronic effective mass is basically unchanged for phonon frequencies in the adiabatic regime. Systematic adiabatic (small- γ) expansions¹⁵ at zero temperature give all contributions of order $\bar{\gamma}$ and correct Eq. (15). However, these contributions come with additional factors $\bar{\Lambda}^n$ ($n \geq 2$). Thus

they are not small close to the polaronic instability and an adiabatic expansion is not possible. This is one reason why the semiclassical approach discussed here is restricted to high to intermediate temperatures which help to re-establish smaller lattice distortions.

The results of Benedetti and Zeyher¹² (although at finite temperatures) for $\gamma = 0.01$ are close to the classical result and fall as they should in the shaded region of Fig. 3. One of the authors has studied the consequences of the isotope shift of Λ_c when both thermal and quantum fluctuations are competing by means of the semiclassical approach revisited here. As one of the most dramatic manifestations an isotope driven insulator-to-metal transition may be observed.¹⁴

V. ADIABATIC CORRECTIONS

From the above considerations it becomes obvious that adiabatic corrections to the classical effective action have to be taken into account. For the Holstein model this has been done in Ref. 14. The idea is to expand the difference $S_{\text{eff}} - S_{\text{class}}$ to second order in $(1 - \delta_{nm}) \underline{W}(\nu_n - \nu_m)$, i.e. to leading order in the non diagonal part of the electron-phonon interaction. This yields

$$S_{\text{eff}} = S_{\text{class}} + S_2 \quad (16)$$

with

$$S_2 = \frac{1}{2T} \sum_{k \neq 0} \vec{Q}(\omega_k) (K + M\omega_k^2) \vec{Q}(\omega_{-k}) + \quad (17)$$

$$\frac{1}{2} \sum_{k \neq 0} \text{Tr}_{\text{orb}} \left[c(\nu_n) - \underline{W}(\vec{Q}) \right]^{-1} \underline{W}[\vec{Q}(\omega_k)]$$

$$\times \left[c(\nu_{n-k}) - \underline{W}(\vec{Q}) \right]^{-1} \underline{W}[\vec{Q}(-\omega_k)]$$

In the following we will present numerical results for the Holstein model at half-filling, i.e. $\underline{W} = gQ$ and $\mu = 0$. We generalize the treatment given in Ref. 14 by using a different numerical implementation which does not rely on approximatively continuing the local electronic Green function from the imaginary to the real frequency axis. Instead, the continuation is done “numerically” exact. This allows for a more extensive discussion of the optical conductivity. We shortly review results from Ref. 14 pertinent to the present work. For $\underline{W} = gQ$ all but one integration in Eq. (5) can be performed analytically and the effective action depends only on the classical coordinate Q

$$S_{\text{eff}}(Q) = S_{\text{class}}(Q) + \sum_{k>0} \ln \left[1 + \frac{\Omega^2(\omega_k, Q)}{\omega_k^2} \right]. \quad (18)$$

Here, not the bare phonon frequency $\Omega^2 = K/M$ enters but a renormalized one which depends on both the classical distortion Q and the even Matsubara frequencies $\omega_k = 2\pi T k$ and reads

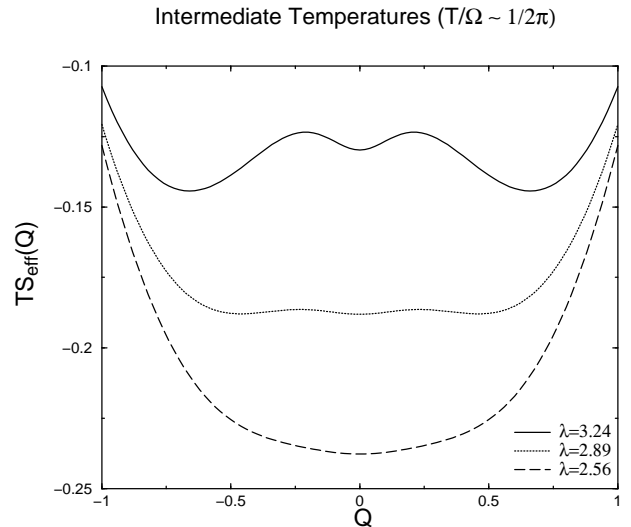


FIG. 4. The effective action S_{eff} as function of the distortion Q for the Holstein model at half-filling. The adiabatic parameter equals $\gamma = 0.2$. Shown is the behavior for different coupling strengths λ at a intermediate temperature of $T/t = 0.036$. The forming of a *triple* (instead of a *double*) well at a finite value of λ is clearly seen.

$$\Omega^2(\omega_k, Q) = \Omega^2 [1 + \Pi(\omega_k, Q)] \quad (19)$$

The ω_k dependence arises from the fact that the phonon propagator is renormalized by electron bubbles, i.e. processes where one electron absorbs (or emits) one phonon and gains (or loses) the energy ω_k . Therefore in Eq. (19)

$$\Pi(\omega_k, Q) = \Lambda T \sum_{\nu_n} \frac{1}{c(\nu_n) - Q} \frac{1}{c(\nu_n - \omega_k) - Q}. \quad (20)$$

If the renormalized phonon frequency were independent of the even Matsubara frequencies $\omega_k = 2\pi T k$, the quantum term S_2 were the action of a harmonic oscillator. This simplification was explored in Ref. 14. Here, however, we will investigate the exact form of the second order quantum corrections.

At weak couplings the mean-field functions $c(\nu_n)$ may be approximated by the free ones. However, at intermediate to strong electron phonon couplings the electronic properties are influenced and the mean-field functions are renormalized as described by the self-consistency equation (7). The local Green function is obtained by the logarithmic derivative of the partition function Z with respect to $c(\nu_n)$, Eq. (6). It reads (denoting $\frac{1}{2} \int dr P(Q)$ by $\langle \rangle$)

$$\mathcal{G}(\nu_n) = \left\langle \frac{1}{c(\nu_n) - Q} + F(\nu_n, Q) \left(\frac{1}{c(\nu_n) - Q} \right)^2 \right\rangle. \quad (21)$$

Comparing to the classical result, the quantum corrections enter in two places. First, they enter in the modified

probability $P(Q) = \exp(-S_{\text{eff}})$ that the classic distortion takes the value Q . Second, they give rise to an additional scattering term $F(\nu_n, Q)$

$$F(\nu_n, Q) = \Lambda T \sum_{k>0} \frac{\Omega^2}{w_k^2 + \Omega_k^2(Q)} \times \left(\frac{1}{c(\nu_{n-k}) - Q} + \frac{1}{c(\nu_{n+k}) - Q} \right) \quad (22)$$

which can be interpreted as generalized Migdal self energy where the classical $k = 0$ term is subtracted. The two modifications have opposing influences. First, as shown in Fig.4, the adiabatic corrections lead to an increased probability for distortions around $Q = 0$ compared to the classical one. In consequence, quantum fluctuations of the lattice (not present in the classical approach) may lead to an increased mobility of the conduction electrons. Second, when an analytic continuation to the real frequency axis of F is performed [yielding $F(\omega, Q)$], a finite imaginary part implies additional electron phonon scattering. Note, that for small frequencies ω below the renormalized one the imaginary part of $F(\omega, Q)$ may be reduced or vanishing.

A. Numerical implementation

Iteration of Eq. (7) and Eq. (21) will yield the local electronic Green function $\mathcal{G}(\nu_n)$ on the imaginary axis. The occurring fermionic and bosonic Matsubara sums are calculated introducing high frequency cut offs $\bar{\omega}$ and $\bar{\nu}$, respectively. The high frequency contributions to the sums are approximated by integrals. For reference we summarize here the results where functions $f(\bar{\omega})$ [$f(\bar{\nu})$] are finite bosonic (fermionic) Matsubara sums up to $\omega_k < \bar{\omega}$ (up to $\nu_n < \bar{\nu}$):

$$S_2(Q) = S_2(Q, \bar{\omega}) + \frac{\Omega}{2T} - \frac{2\Omega}{2\pi T} \arctan \frac{\bar{\omega}}{\Omega} - \frac{\bar{\omega}}{2\pi T} \ln \left(1 + \frac{\Omega^2}{\bar{\omega}^2} \right) \quad (23)$$

$$\Pi(\omega_k, Q) = \Pi(\omega_k, Q, \bar{\nu}) - \frac{1}{2\pi\omega_k} \ln \left(1 + \frac{2\bar{\nu}\omega_k + \omega_k^2}{Q^2 + \bar{\nu}^2} \right) \quad (24)$$

$$F(\nu_n, Q) = F(\nu_n, Q, \bar{\omega}) + \frac{\Lambda\Omega}{\pi} \frac{1}{Q^2 - \Omega^2} \times \left[Q \left(\arctan \frac{\bar{\omega}}{\Omega} - \frac{\pi}{2} \right) - \Omega \left(\arctan \frac{\bar{\omega}}{Q} - \text{sgn} Q \frac{\pi}{2} \right) \right]. \quad (25)$$

In principle, the truncation at $\bar{\omega}$ and the adding of an asymptotic contribution in Eq. (25) is not valid if $\nu_n \approx \bar{\omega}$, i.e. for large values of the fermionic Matsubara frequency. However, the quantum scattering term $F(\nu_n, Q)$ tends to zero in this case and small errors are not important. In all

our calculations we used 128 bosonic (fermionic) Matsubara frequencies. To speed up the integration performed in Eq. (21) the electron electron bubble $\Pi(\omega_k, Q)$ has been interpolated as function of Q for each value of ω_k in each DMFT iteration step.

In the present approach only one dimensional integrals over a real variable have to be calculated. This can be done with high precision yielding $\mathcal{G}(\nu_n)$ up to 14 digits. Therefore, we can continue the electronic Green function to the real frequency axis employing a “simple” Padé approximation.¹⁷ The quality of the results are even more improved when using the classical solution as a reference state, i.e. doing the continuation for the difference $\mathcal{G} - \mathcal{G}_{\text{class}}$. This is a real strength of the present semiclassical approach allowing the calculation of dynamic quantities without further assumptions. As important example we have calculated here the finite temperature optical conductivity of the Holstein model as convolution of two full Green functions:

$$\sigma(\Omega) = \sigma_0 \int d\omega \left(-\frac{f(\omega + \Omega) - f(\omega)}{\Omega} \right) \times \int d\epsilon \rho_0(\epsilon) \rho(\epsilon, \omega) \rho(\epsilon, \omega + \Omega). \quad (26)$$

The external frequency Ω shall not be confused with the phonon frequency. In Eq. (26) is $\rho_0(\epsilon)$ of semicircular form and the spectral function defined by

$$\rho(\epsilon_{\vec{k}}, \omega) = -\frac{1}{\pi} \text{Im} \left[\frac{1}{\omega + \mu - \Sigma(\omega) - \epsilon_{\vec{k}}} \right]. \quad (27)$$

The self-energy $\Sigma(\omega)$ can be obtained from the local electronic Green function $\mathcal{G}(\omega)$ on the real frequency axis. We also present results for the density of states

$$\rho(\omega) = \int d\epsilon \rho_0(\epsilon) \rho(\epsilon, \omega). \quad (28)$$

To summarize, our implementation of the semiclassical approach for the Holstein model differs in two way from the one discussed in Ref. 14. First, when calculating the effective action Eq. (17) we do not rely on a static approximation, i.e. we do not replace $\Omega(\omega_k, Q) \rightarrow \Omega(0, Q)$. However, this has little influence on the results. Second and most important, $\mathcal{G}(\nu_n)$ is continued to the real axis not approximatively but numerically exact. In particular, the investigations of dynamic quantities for electron-phonon couplings above the (classical) polaronic instability is possible which is not achieved in Ref. 14.

B. Limitations

Before presenting results we shortly summarize the shortcomings of the presented semiclassical approach as discussed extensively in Ref. 14. Within the framework of dynamical mean-field theory the approach becomes exact at high temperatures $T \rightarrow \infty$, irrespectively which

value the electron phonon coupling takes. However, at low temperatures the approach fails for two reasons:

First, at intermediate to strong couplings the weak coupling (Fermi liquid) ground state is fundamentally reconstructed. In the present formalism this is reflected by the occurrence of imaginary phonon frequencies $\Omega^2(\omega_k, Q)$. In this case $S_2(Q)$ is not well defined anymore at low temperatures. Only larger temperatures re-stabilize the ground state. To explore this in more detail, let us suppose the renormalized phonon frequency $|\Omega(\omega_k = 0, Q = 0)|$ turns imaginary at a critical coupling Λ_c . For $T \rightarrow 0$ and for couplings just above the critical value $\Delta\Lambda = \Lambda - \Lambda_c$ one finds $\Omega^2(0, 0) = -\Omega^2 \Delta\Lambda / \Lambda_c$.¹⁴ Because $\Omega^2(\omega_k, Q)$ is a strictly monotonic decreasing function with Matsubara frequency and displacement, the quantum correction $S_2(Q)$ is only defined if

$$T > \frac{\Omega}{2\pi} |\Omega(0, 0)| = \frac{\Omega}{2\pi} \sqrt{\frac{\Delta\Lambda}{\Lambda_c}}. \quad (29)$$

However, at high temperatures $\Omega^2(0, 0) = \Omega^2 - \Lambda/(4T)$ and the renormalized phonon frequency is always real.

Second, also at weak couplings the ground state cannot be reached. A purely classical approximation ($\Omega \rightarrow 0$) would lead to a T -linear scattering rate with coefficient of order unity. The semiclassical approximation overcorrects for this behavior, cancelling the leading term leaving a correction of order γT but of the wrong sign. Note that for $T < \Omega$ this is $\mathcal{O}(\gamma^2)$. Note also that at $T = 0$ the adiabatic expansion is possible for weak couplings (see Sec. IV and Ref. 15).

In conclusion the semiclassical approach is restricted to a range of high ($T/\Omega \gg 1/2\pi$) to intermediate ($T/\Omega \sim 1/2\pi$) temperatures and we present only results in this range.

C. Results

In the following we present numerical results for the density of states (DOS) and the optical conductivity at finite temperatures for electron-phonon couplings from weak to strong. The model under consideration is the Holstein model with one (spinless) electron per each two sites (half filling), i.e. we discuss the simplest case of non-degenerate electrons coupling linearly to non-degenerate lattice distortions.

In Fig. 5 we show typical results at *weak* couplings, i.e. for values of Λ well below the (classical) polaronic instability of $\Lambda_c \approx 2.36$. We recover the behavior known from calculations employing Migdal-Eliashberg theory.¹⁸ A tiny quasi-particle peak at zero frequency (and the inset in the upper panel showing the DOS over the complete frequency range shall demonstrate that it is indeed a tiny structure) is observed in the DOS and *no* upper and lower sub-bands are formed. The quasi-particle peak originates from the fact that conduction electrons can only inelastically scatter from quantum lattice fluctuations with a fi-

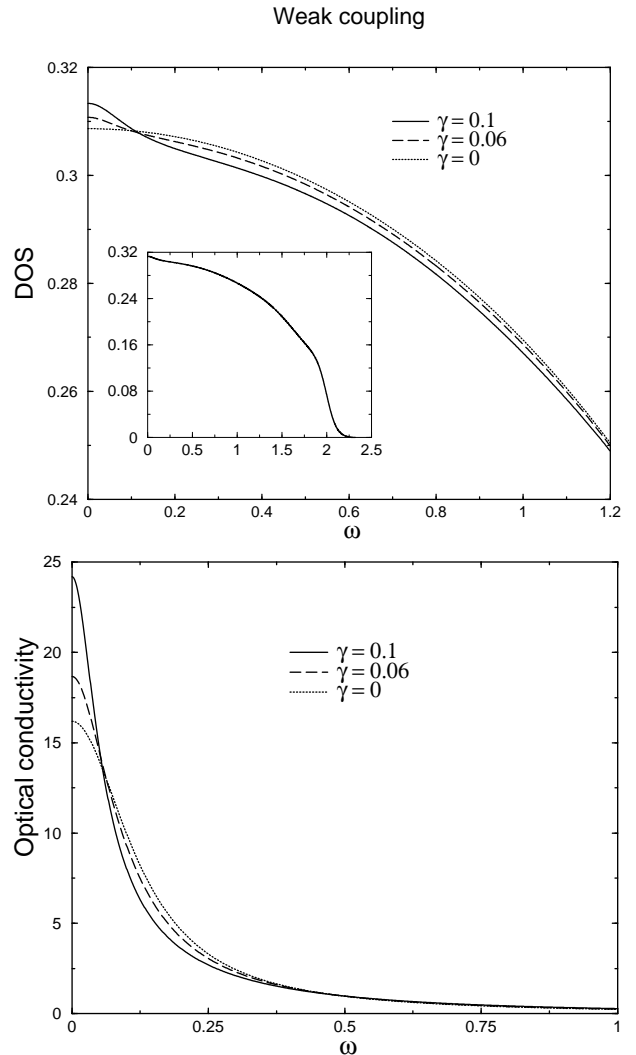


FIG. 5. UPPER PANEL: DOS of the Holstein model (half-filling) at a *weak* electron-phonon coupling $\lambda = 1$ and a temperature $T/t = 0.04$. Results for various values of the adiabatic parameter γ are shown. For finite phonon frequencies a small quasi-particle peak is visible at $\omega = 0$. The inset displays the DOS over the full frequency range for the largest value of the adiabatic parameter, $\gamma = 0.1$. On this scale the quasiparticle peak is hardly seen. LOWER PANEL: The frequency dependent optical conductivity for the same model and parameters as in the upper panel. It displays a Drude-like behavior.

nite frequency transfer. Therefore, the peak gets slightly broader with increasing adiabatic parameter γ . Note that in all our calculations γ is a small parameter. Following the behavior of the DOS, the optical conductivity shows a typical metallic behavior with a sharp Drude peak. The optical conductivity drops monotonically with increasing applied frequency ω .

Fig. 6 shows the DOS and the optical conductivity at an *intermediate* electron-phonon coupling, just above the (classical) polaronic instability. In this regime isotope effects (i.e. changing values of γ) may alter the behavior *qualitatively*. At low phonon frequencies sub-bands in the DOS are weakly developed. With increasing γ these sub-bands disappear in favor of a quasi-particle peak at $\omega = 0$. The quasi-particle peak is more pronounced as in the weak coupling case with slightly smaller width. With increasing adiabatic parameter also the behavior of the optical conductivity changes qualitatively from an insulating behavior with increased *intra-band* absorption to a Drude-like metallic behavior with an *incoherent contribution* visible as “shoulder”. Although a Drude peak develops the conductivity is one order of magnitude smaller than for small electron-phonon couplings. One may speak of a “bad metal”.

Results for *stronger* couplings are shown in Fig. 7. Sub-bands are well developed in both the DOS and the optical conductivity. Only for a significant change in the phonon frequency a Drude-like metallic behavior is restored. In this sense isotope effects are less pronounced in the strong coupling case as in the intermediate one as they do not lead to immediate qualitative changes. The qualitative behavior as given in the classical picture is maintained for all small values of the adiabatic parameter γ . However, at larger phonon frequencies both a quasi-particle peak at $\omega = 0$ and sub-bands are visible simultaneously, a feature which cannot be obtained within Migdal-Eliashberg theory. The intra-band absorption in the optical conductivity occurs around $\omega \approx \Lambda$ and shifts to smaller frequencies with increasing value of the adiabatic parameter. The intra-band absorption is asymmetric about its peak. In particular, the low-frequency side of the absorption peak is elevated above the high-frequency side.

The low temperature behavior of the DOS and the optical conductivity in the adiabatic regime has been carefully studied by Benedetti and Zeyher.¹² Their results confirm nicely that our findings at intermediate temperatures are not spoiled by the low temperature break down of the semiclassical approach but that they reflect the physical behavior of the model. In particular, the optical conductivity shows the behavior presented here: (i) Drude like behavior at weak coupling, (ii) quasi-particle peak together with incoherent features at intermediate couplings and (iii) intra-band absorption at strong coupling. Obviously, the present semiclassical approach is capable of describing the interesting crossover regime from high to low temperatures. Unfortunately, isotope effects on the optical conductivity

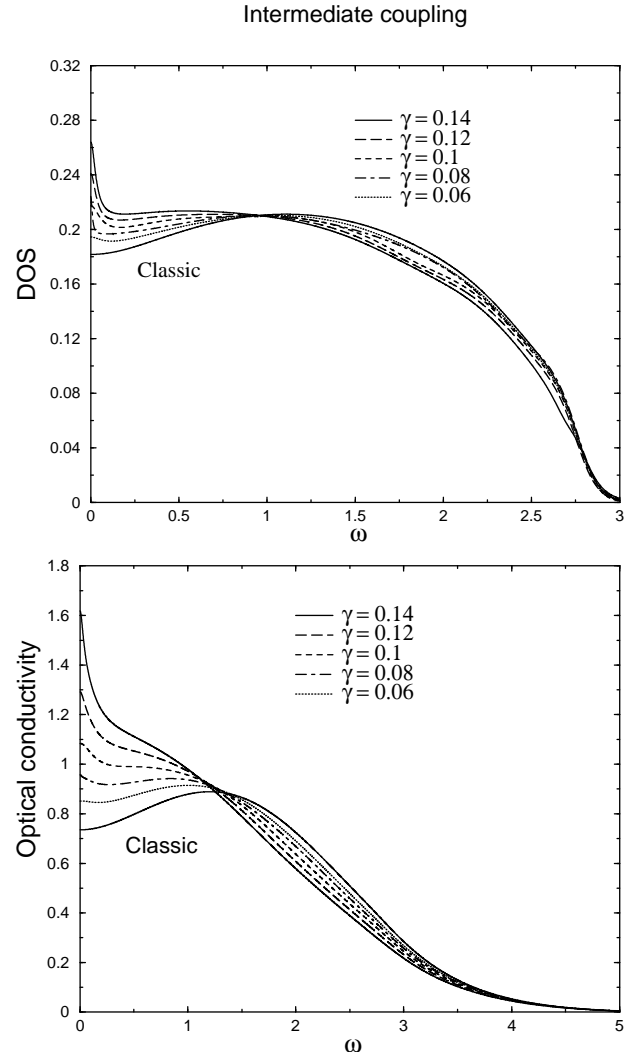


FIG. 6. UPPER PANEL: DOS of the Holstein model (half-filling) at an *intermediate* electron-phonon coupling $\lambda = 2.89$ and a temperature $T/t = 0.04$. Results for various values of the adiabatic parameter γ are shown. Increasing the adiabatic parameter has a considerable influence. Weakly developed sub-bands occurring at small phonon frequencies disappear in favour of a narrow quasi-particle peak at $\omega = 0$ with increasing γ . LOWER PANEL: The frequency dependent optical conductivity for the same model and parameters as in the upper panel. At small phonon frequencies an intra-band absorption is clearly visible. With increasing phonon frequency this feature merges with a developing Drude peak giving rise to a “shoulder”.

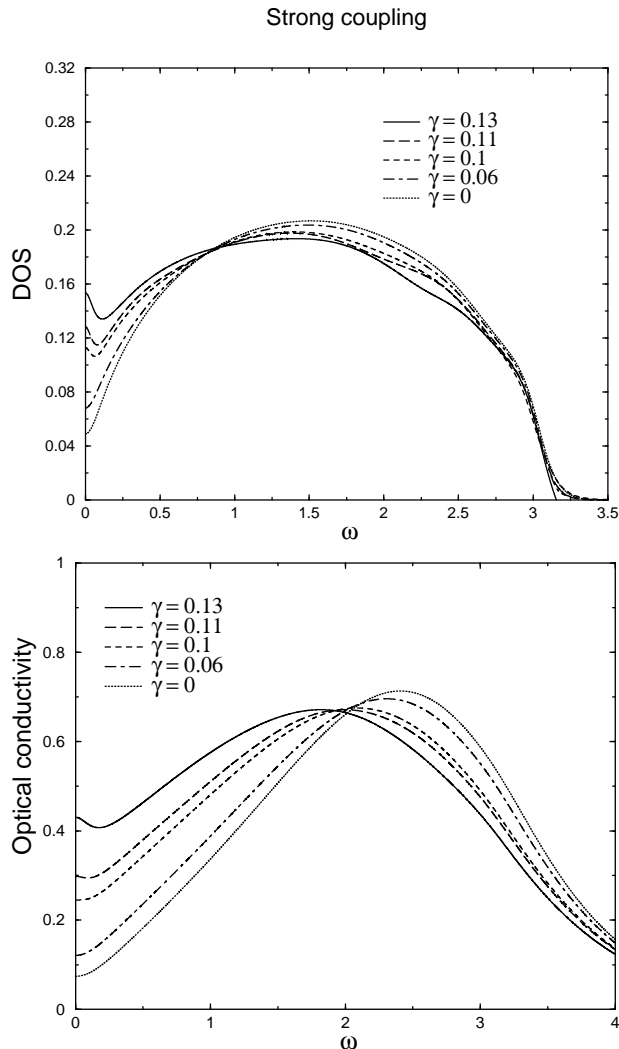


FIG. 7. UPPER PANEL: DOS of the Holstein model (half-filling) at a *strong* electron-phonon coupling $\lambda = 3.24$ and a temperature $T/t = 0.04$. Results for various values of the adiabatic parameter γ are shown. For all values of γ the DOS displays well developed sub-bands. A quasi-particle peak becomes visible for larger values of the phonon frequency. LOWER PANEL: The frequency dependent optical conductivity for the same model and parameters as in the upper panel. An asymmetric inter-band absorption is clearly seen situated roughly at $\omega \approx \Lambda$, shifting towards smaller frequencies with increasing γ .

were not discussed in Ref. 12 which are especially relevant when Migdal-Eliashberg theory breaks down (i.e. at intermediate electron-phonon coupling strengths).

It should be noted that the qualitative features and changes in the optical conductivity when increasing the electron-phonon coupling from weak to strong are similar to the ones predicted by a *small-polaron* absorption theory.¹⁹ However, in this theory the hopping of the conduction electrons is a small parameter contrary to the approach discussed here which is based on an adiabatic expansion. Therefore a comparison is only meaningful in the limit of large electron-phonon couplings where small polarons are well defined quasi-particles. Here, the main absorption process is the excitation of a self-trapped electron from its localized state at one site to a localized state at a neighboring one. Due to thermal and quantum fluctuations of the lattice the energies of the localized states are broadened and one obtains for the optical conductivity

$$\sigma \sim \frac{1}{\omega} \exp[-(\Lambda - \omega)^2 / (4 \Lambda E_{\text{vib}})] \quad (30)$$

where $E_{\text{vib}} = \Omega/2$ is the zero-point vibrational energy at low temperatures and $E_{\text{vib}} = T$ in the case of high enough temperatures when the vibrations can be treated classically. The classical (high temperature) result can be compared to our numerical data in the strong coupling limit and reasonable agreement is found.

Depending on the values of the phonon frequency Ω and coupling strength Λ qualitative features of various experiments are present. To name two examples: (i) In $\text{Ba}_{1-x}\text{K}_x\text{BiO}_3$ for high enough doping x (so that charge ordering is destroyed) the optical conductivity displays a Drude-like peak with a pronounced incoherent feature in the mid infrared;¹ (ii) Asymmetric intra-band absorption can be observed in the alkali doped fullerenes K_3C_{60} and Rb_3C_{60} .² As outlined in this paper the semiclassical approach can be extended to more realistic models of electrons in degenerate orbital states coupling to Jahn-Teller distortions allowing for a more detailed analysis of experiments. Along the lines of Refs. 13 and 20 effects of *local* Coulomb repulsion may be included.

VI. CONCLUSION

In this paper we have extended a semiclassical approach¹⁴ based on the dynamical mean-field theory recently introduced by one of the authors to treat the coupling of conduction electrons to local Jahn-Teller distortions in metals and metallic molecular crystals. We have improved previous numerical treatments allowing a detailed discussion of dynamic quantities such as the finite temperature optical conductivity and presented results for the simplifying Holstein model. In particular, the density of states and the optical conductivity could be studied not only for electron-phonon couplings below

the (classical) polaronic instability but also above. At intermediate to strong couplings the optical conductivity displays features which are known from experiments on phonon mediated superconductors with high transition temperatures. Depending on parameters, a Drude-like peak with a pronounced incoherent “shoulder” or an asymmetric intra-band absorption is observed. Strong isotope effects occur at couplings close to the polaronic instability changing the qualitative behavior of the system.

The presented results demonstrate that the analysis of simplified effective actions based on the dynamical mean-field theory and adiabatic expansions is a powerful tool to study the influence of local lattice fluctuations on electronic properties of metals. Future work will reveal if the presented approach is capable also of a *quantitative* analysis of electronic properties of metals and metallic molecular crystals strongly influenced by local Jahn-Teller distortions.

Acknowledgements S.B. thanks A. Millis for many useful and stimulating discussions. S.B. acknowledges the Niedersachsen-Israel foundation for financial support at early stages of this work.

-
- ¹ A.V. Puchkov, T. Timusk, M.A. Karlow, S.L. Cooper, P.D. Han and D.A. Payne, Phys. Rev. B **54**, 6686 (1996)
 - ² L. Degiorgi, E.J. Nicol, O. Klein, G. Grüner, P. Wachter, S.M. Huang, J. Wiley and R.B. Kaner, Phys. Rev. B **49**, 7012 (1994)
 - ³ O. Gunnarsson, Rev. Mod. Phys. **69**, 575 (1997)
 - ⁴ A.B. Migdal, Sov. Phys. JETP **7**, 996 (1958); G.M. Eliashberg, Sov. Phys. JETP **11**, 696 (1960)
 - ⁵ A.S. Alexandrov, V.V. Kabanov and D.K. Ray, Phys. Rev. B **49**, 9915 (1994)
 - ⁶ I.G. Lang and Yu.A. Firsov, Sov. Phys. JETP **16**, 1301 (1963)
 - ⁷ A. Georges, G. Kotliar, W. Krauth and M.J. Rozenberg, Rev. Mod. Phys. **68**, 13 (1996)
 - ⁸ S. Ciuchi, F. de Pasquale, S. Fratini and D. Feinberg, Phys. Rev. B **56**, 4494 (1997)
 - ⁹ J.K. Freericks, M. Jarrell, D.J. Scalapino, Phys. Rev. B **48**, 6302 (1993); J.K. Freericks and M. Jarrell, Phys. Rev. B **50**, 6939 (1994); J.K. Freericks, V. Zlatić, W. Chung and M. Jarrell, Phys. Rev. B **58**, 11613 (1998)
 - ¹⁰ D. Meyer, A.C. Hewson and R. Bulla, Phys. Rev. Lett. **89**, 196401 (2002)
 - ¹¹ A.J. Millis, R. Mueller and B.I. Shraiman, Phys. Rev. B **54**, 5389 (1996). A.J. Millis, R. Mueller and B.I. Shraiman, Phys. Rev. B **54**, 5405 (1996)
 - ¹² P. Benedetti and R. Zeyher, Phys. Rev. B, **58**, 14320 (1998)
 - ¹³ A. Deppeler and A.J. Millis, Phys. Rev. B **65**, 100301 (2002)
 - ¹⁴ S. Blawid, A. Deppeler and A.J. Millis, Phys. Rev. B **67**, 165105 (2003)
 - ¹⁵ A. Deppeler and A.J. Millis, Phys. Rev. B **65**, 224301 (2002)
 - ¹⁶ C.C. Chancey and M.C.M. O’Brien, *The Jahn-Teller effect in C₆₀ and other icosahedral complexes* (Princeton University Press, 1997)

- ¹⁷ H.J. Vidberg and J.W. Serene, J. Low Temp. Phys. **29**, 179 (1977)
- ¹⁸ J.P. Hague and N. d’Ambrumenil, cond-mat/0106355 (unpublished)
- ¹⁹ D. Emin, Phys. Rev. B **48**, 13691 (1993)
- ²⁰ A. Deppeler and A.J. Millis, cond-mat/0204617